Rustrela Virus as Putative Cause of Nonsuppurative Meningoencephalitis in Lions

Madeleine de le Roi, Christina Puff, Peter Wohlsein, Florian Pfaff, Martin Beer, Wolfgang Baumgärtner, Dennis Rubbenstroth

Retrospective investigation of archived tissue samples from 3 lions displaying nonsuppurative meningoencephalitis and vasculitis led to the detection of rustrela virus (RusV). We confirmed RusV antigen and RNA in cortical neurons, axons, astrocytes and Purkinje cells by reverse transcription quantitative PCR, immunohistochemistry, and in situ hybridization.

Until recently, rubella virus (RuV), an RNA virus with single-stranded RNA genome of positive orientation, was considered the only virus of the genus *Rubivirus* and the family *Matonaviridae* (*1*–*3*). Two close relatives of RuV, designated rustrela virus (RusV) and ruhugu virus (RuhV), were discovered in animals in 2020. RusV was demonstrated to cause nonsuppurative meningoencephalitis in a range of zoo animals in Germany (*1*,*4*,*5*). Furthermore, RusV was detected in domestic cats (*Felis catus*) showing clinical signs of staggering disease in Germany, Austria, and Sweden (*6*). Wild yellow-necked field mice (*Apodemus flavicollis*) and wood mice (*Apodemus sylvaticus*) are assumed to be reservoir hosts of RusV (*1*,*4*,*6*).

In the 1970s and 1980s, a series of fatal nonsuppurative encephalitis cases of undetermined cause had occurred in lions (*Panthera leo*) and tigers (*Panthera tigris*) kept in zoological gardens in Germany (*7*,*8*). We reinvestigated cases of 3 lions with nonsuppurative meningoencephalitis of unknown etiology from the 1980s for the presence of RusV.

The etiology of meningoencephalitides remains undetermined in many cases (*6*,*9*); a possible explanation is that conventional methods based on the recognition of virus-specific proteins and nucleic acids did not detect viral variants. Immunohistochemical detection of double-stranded RNA (dsRNA) is considered a virus-sensing tool irrespective of the particular virus (*10*). Therefore, we assessed the applicability of antibodies sensing dsRNA as an alternative virus detection method.

Author affiliations: University of Veterinary Medicine Hannover Foundation, Hannover, Germany (M. de le Roi, C. Puff, P. Wohlsein, W. Baumgärtner); Friedrich-Loeffler-Institut, Greifswald-Insel Riems, Germany (F. Pfaff, M. Beer, D. Rubbenstroth)

DOI: https://doi.org/10.3201/eid2905.230172

The Study

We retrospectively investigated 3 lions for the presence of RusV. The lions were identified in 2 zoos in northern and western Germany; they exhibited neurologic signs and nonsuppurative meningoencephalitis. Lion 1 died in 1980 in a zoo in Lower Saxony, whereas lions 2 and 3 were submitted for pathological examination in 1989 by a zoo in North Rhine-Westphalia. All 3 lions displayed a mild, multifocal, lymphohistiocytic meningoencephalitis and vasculitis (Figure 1, panel A) and occasional glial nodules. Inflammatory infiltrates were most prominent in the cerebral gray matter and less prominent in cerebral white matter, cerebellum, and meninges. The spinal cord was not available for analysis. We tested archived formalin-fixed, paraffin-embedded (FFPE) tissues for the presence of RusV RNA and antigen by quantitative reverse transcription PCR (qRT-PCR), in situ hybridization (ISH) and immunohistochemistry (IHC). We included FFPE tissues originating from 8 lions without nonsuppurative meningoencephalitis (lions 4–11) as controls (Appendix, https://wwwnc.cdc.gov/EID/article/29/5/23-0172-App1.pdf).

FFPE brain samples from lions 1–3 tested positive for RusV RNA by the broadly reactive qRT-PCR assay panRusV-2 (*6*). Cycle quantification (Cq) values were 29–38. We detected no RusV RNA in central nervous system (CNS) samples from any of the 8 control animals (Appendix Table 1).

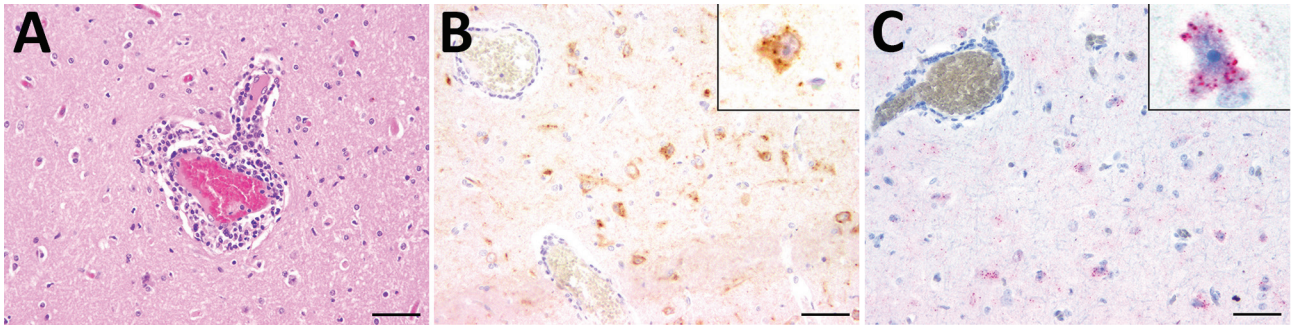

Figure 1. Histopathologic, immunohistochemical, and in situ hybridization findings in the cerebrum of a lion tested positive for rustrela virus (RusV) by quantitative reverse transcription PCR. A) Histopathologic analysis of cerebral sample from lion 3 indicated lymphohistiocytic meningoencephalitis and vasculitis. B) Immunohistochemistry analysis showed RusV antigen in cortical neurons and their processes. Cytoplasmic granular immunoreactivity is visible (inset). C) In situ hybridization revealed RusV RNA in cortical neurons; we observed cytoplasmic granular-positive signal (inset). Scale bars indicate 50 μm.

We determined a partial host-genome RusV sequence 409 bp long for all 3 RusV-positive animals by Sanger sequencing of overlapping RT-PCR products (Appendix). The sequences shared 97.8% nucleotide identity; phylogenetic analysis revealed all 3 sequences to form a single clade together with the sequence from a domestic cat in Hannover, Lower Saxony, in 2017 (*6*). Of note, this subclade was more closely related to sequences from cats with staggering disease in Austria than to sequences from zoo animals, domestic cats, and wild rodents in northeastern Germany (Figure 2).

IHC investigation for the presence of RusV capsid antigen using monoclonal antibody 2H11B1 (*6*) revealed multifocal, cytoplasmic, granular reactions, predominantly in cerebral cortical perikarya and their axons, in few astrocytes as well as in Purkinje cells of all 3 PCR-positive lions (Figure 1, panel B). Likewise, we detected RusV-specific RNA using a newly designed ISH probe (Appendix) in the brains of lions 2 and 3, but not of lion 1. We found viral RNA as a cytoplasmic granular signal in cortical perikarya (Figure 1, panel C). We observed RusV-specific capsid antigen and RNA in cerebral cortical neurons adjacent to perivascular infiltrates and also in neurons in more distant areas not associated with inflammatory changes. Neither IHC nor ISH revealed positive signals in any of the examined peripheral organs of the 3 RusV-positive animals and RusV-negative lion 7 (Appendix Table 1) or in the CNS of control animals. IHC staining for dsRNA using the dsRNA antibodies K1 and J2 (*11*) provided positive results in the CNS of all tested animals (Appendix Table 1). Immunolabeling with anti-dsRNA antibody 9D5 (*11*) remained negative for all 3 RusV-positive animals, whereas the RusV-negative lions 7 and 9 tested positive (Appendix Table 1).

Conclusions

The results of this study strongly indicate RusV as the potential cause of fatal lymphohistiocytic meningoencephalitis in lions from Germany in the 1980s. The animals were reported to have had neurologic disorders characterized by fever, depression, ataxia, and prolapse of the tongue (*7*). These clinical and histopathological findings are similar to those described previously for RusV-infected zoo animals and domestic cats (*1*,*4*–*6*); they also resemble RuV-induced encephalitis in humans (*12*).

A partial colocalization of RusV antigen and RNA detection with histopathologic lesions has been observed previously (*1*,*4*,*6*). Although the pathogenesis of RusV infection has not been elucidated, a virally triggered immune response that remains present even after focal virus clearance may provide an explanation for this phenomenon (*13*). In addition, vasculitis caused by a type III hypersensitivity reaction should be considered.

The lack of viral antigen and RNA in organs other than the CNS of the infected lions is consistent with previous findings in RusV-infected zoo animals of other species, in which RusV RNA was predominantly detected in the CNS and only sporadically in other organs (*1*,*4*,*5*). These results indicate a strong neurotropism of RusV also in lions.

In this study, we consistently detected RusV RNA and antigen in the affected animals using 3 independent methods (qRT-PCR, ISH, and IHC). The lack of viral RNA detection by ISH in the brain of lion 1, positive by qRT-PCR, could be a result of lower sensitivity of ISH (*14*) or of a higher degree of RNA degradation in this >40-year-old sample. Furthermore, the crosslinking of proteins caused by formalin has been shown to influence the quality and accessibility of DNA or RNA in FFPE material (*15*).

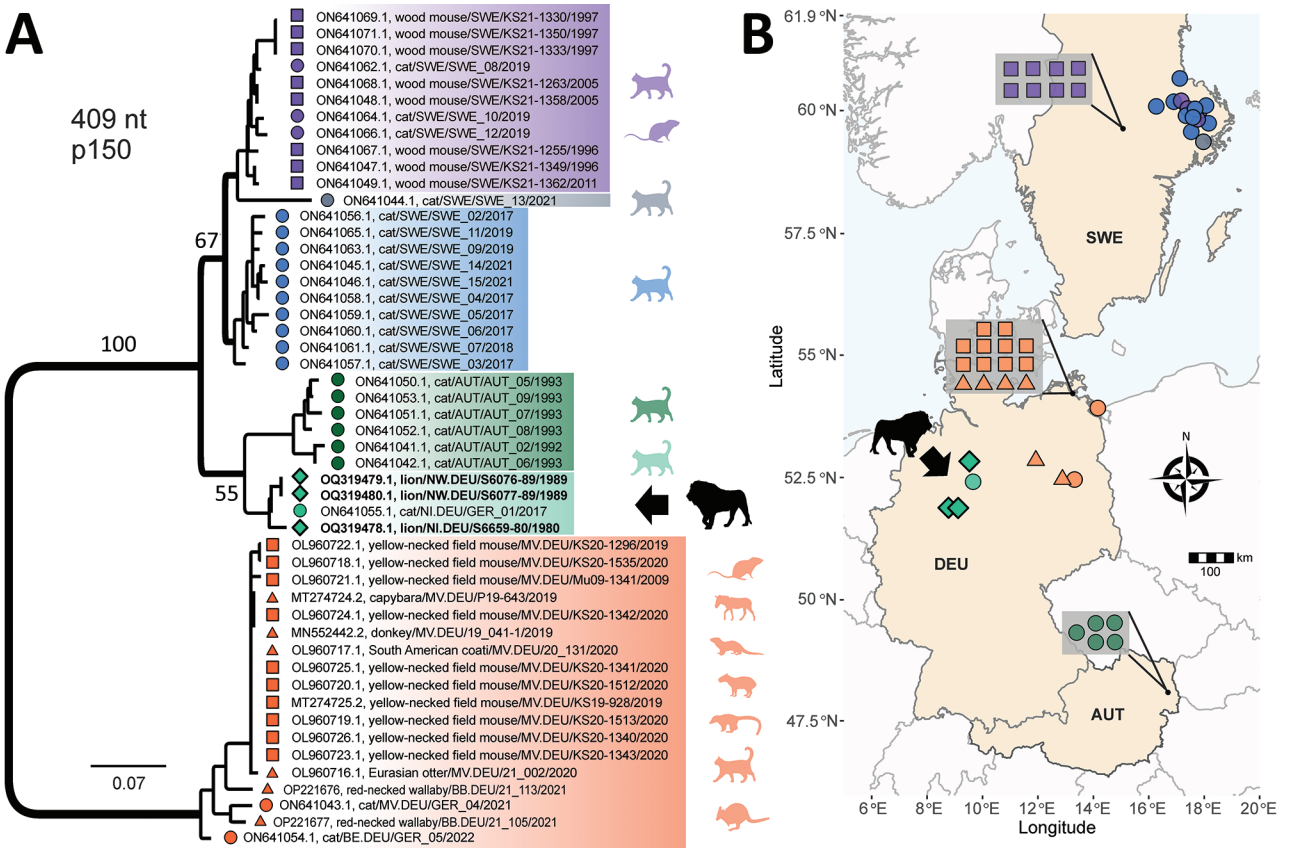

Figure 2. Phylogenetic analysis and spatial distribution of rustrela virus infections in Europe. A) Maximum-likelihood phylogenetic tree of partial rustrela virus (RusV) sequences (409 nt, representing genome positions 100–508 of donkey-derived RusV reference genome, GenBank accession no. MN552442.2). Only bootstrap values at major branches are shown in the phylogenetic tree. RusV sequence names are shown in the format host/ISO 1366 code of location (federal, state, country)/animal ID/year. The tree was produced using IQ-TREE version 2.2.0; transition model 2 plus empirical frequency plus gamma 4 with 1,000 bootstrap replicates. Bold text indicates sequences from this study. Scale bar indicates substitutions per site. B) Mapping of the geographic origin of RusV-positive animals in Europe. Colors represent the phylogenetic clades of the sequences. Diamonds represent lions; circles, domestic cats; triangles, other zoo animals; squares, *Apodemus* spp. rodents. Symbols in gray boxes represent individuals from the same or very close locations. AUT, Austria; BE, Berlin; DEU/GER, Germany; MV, Mecklenburg–Western Pomerania; NI, Lower Saxony; NW, North Rhine–Westphalia; SWE, Sweden.

Immunohistochemical investigation for dsRNA revealed positive results in the brains of all investigated lions, regardless of their RusV infection status. Although it is possible that the RusV-negative lions were infected by other neurotropic RNA viruses, this scenario appears unlikely because no CNS lesions were observed in control animals 4–11. Thus, this method appears unsuitable for reliable detection of viral dsRNA in the brains of lions and perhaps other animals.

In summary, our study reveals that RusV was present in northern and western Germany in the 1980s. Detecting RusV in lions indicates an even broader host range of RusV, encompassing a variety of different species (*1*,*4*–*6*) and suggests that other wild and captive felids may be susceptible to RusV infection. As described previously (*6*), fulfilling Henle-Koch's postulates by experimental reproduction of the disease has not been possible because of lack of RusV isolates. Nevertheless, the association between RusV detection and disease demonstrated in this study, combined with previous studies on RusV infections in zoo animals and domestic cats, strongly suggests RusV as a causative agent of meningoencephalitis in lions.

Acknowledgments

We thank Julia Baskas, Petra Grünig, Jana-Svea Harre, Claudia Herrmann, Weda Hoffmann, Kerstin Rohn, Kerstin Schöne, Caroline Schütz, Philip Starcky, Kathrin Steffen, Danuta Waschke, and Melanie Woischnik for technical assistance. We are also grateful to Andrea Aebischer for providing the RusV-specific monoclonal antibody 2H11B1.

This work was in part supported by the Deutsche Forschungsgemeinschaft (DFG; German Research Foundation; -398066876/GRK 2485/1-VIPER-GRK) and by the German Federal Ministry of Education and Research, project RubiZoo (grant no. 01KI2111).

About the Author

Ms. de le Roi is a PhD student in the Department of Pathology at the University of Veterinary Medicine Hannover Foundation, Hannover, Germany. Her research field focuses on alternative virus detection methods.

References

1. Pfaff F, Breithaupt A, Rubbenstroth D, Nippert S, Baumbach C, Gerst S, et al. Revisiting rustrela virus: new cases of encephalitis and a solution to the capsid enigma. Microbiol Spectr. 2022;10:e0010322. https://doi.org/10.1128/spectrum.00103-22
2. Mankertz A, Chen MH, Goldberg TL, Hübschen JM, Pfaff F, Ulrich RG; ICTV Report Consortium. ICTV virus taxonomy profile: *Matonaviridae* 2022. J Gen Virol. 2022;103. In press. https://doi.org/10.1099/jgv.0.001817
3. Parkman PD, Buescher EL, Artenstein MS. Recovery of rubella virus from army recruits. Proc Soc Exp Biol Med. 1962;111:225–30. https://doi.org/10.3181/00379727-111-27750
4. Bennett AJ, Paskey AC, Ebinger A, Pfaff F, Priemer G, Höper D, et al. Relatives of rubella virus in diverse mammals. Nature. 2020;586:424–8. https://doi.org/10.1038/s41586-020-2812-9
5. Voss A, Schlieben P, Gerst S, Wylezich C, Pfaff F, Langner C, et al. Rustrela virus infection—an emerging neuropathogen of red-necked wallabies (*Macropus rufogriseus*). Transbound Emerg Dis. 2022;69:4016–21. https://doi.org/10.1111/tbed.14708
6. Matiasek K, Pfaff F, Weissenböck H, Wylezich C, Kolodziejek J, Tengstrand S, et al. Mystery of fatal "staggering disease" unravelled: novel rustrela virus causes severe meningoencephalomyelitis in domestic cats. Nat Commun. 2023;14:624. https://doi.org/10.1038/s41467-023-36204-w
7. Truyen U, Stockhofe-Zurwieden N, Kaaden OR, Pohlenz J. A case report: encephalitis in lions. Pathological and virological findings. Dtsch Tierarztl Wochenschr. 1990;97:89–91.
8. Flyr K. Encephalomyelitis bei Großkatzen. Dtsch Tierarztl Wochenschr. 1973;80:393–416.
9. Nessler J, Wohlsein P, Junginger J, Hansmann F, Erath J, Söbbeler F, et al. Meningoencephalomyelitis of unknown origin in cats: a case series describing clinical and pathological findings. Front Vet Sci. 2020;7:291. https://doi.org/10.3389/fvets.2020.00291
10. Koyama S, Ishii KJ, Coban C, Akira S. Innate immune response to viral infection. Cytokine. 2008;43:336–41. https://doi.org/10.1016/j.cyto.2008.07.009
11. Störk T, de le Roi M, Haverkamp AK, Jesse ST, Peters M, Fast C, et al. Analysis of avian Usutu virus infections in Germany from 2011 to 2018 with focus on dsRNA detection to demonstrate viral infections. Sci Rep. 2021;11:24191. https://doi.org/10.1038/s41598-021-03638-5
12. Frey TK. Neurological aspects of rubella virus infection. Intervirology. 1997;40:167–75. https://doi.org/10.1159/000150543
13. Zdora I, Raue J, Söbbeler F, Tipold A, Baumgärtner W, Nessler JN. Case report: lymphohistiocytic meningoencephalitis with central nervous system vasculitis of unknown origin in three dogs. Front Vet Sci. 2022;9:944867. https://doi.org/10.3389/fvets.2022.944867
14. Pfankuche VM, Hahn K, Bodewes R, Hansmann F, Habierski A, Haverkamp AK, et al. Comparison of different in situ hybridization techniques for the detection of various RNA and DNA viruses. Viruses. 2018;10:384. https://doi.org/10.3390/v10070384
15. Bodewes R, van Run PR, Schürch AC, Koopmans MP, Osterhaus AD, Baumgärtner W, et al. Virus characterization and discovery in formalin-fixed paraffin-embedded tissues. J Virol Methods. 2015;214:54–9. https://doi.org/10.1016/j.jviromet.2015.02.002

Address for correspondence: Dennis Rubbenstroth, Friedrich-Loeffler-Institut, Südufer 10, 17493 Greifswald-Insel Riems, Germany; email: Dennis.Rubbenstroth@fli.de

Article DOI: https://doi.org/10.3201/eid2905.230172

Rustrela Virus as Putative Cause of Nonsuppurative Meningoencephalitis in Lions

Appendix

Materials and Methods

Animals

Archived formalin-fixed, paraffin-embedded (FFPE) material originated from 11 lions (*Panthera leo*) (Appendix Table 1). All 11 animals had been submitted from 1980 to 2022 by zoological institutions from northern and western Germany (federal states Lower Saxony and North Rhine-Westphalia) for pathological examination. Lions 1 to 3 had been selected due to the diagnosis of nonsuppurative meningoencephalitis. Lions 2 and 3 had been previously described by Truyen et al. (*1*). Lions 4 to 11 did not show signs of a nonsuppurative meningoencephalitis and were included as control animals (Appendix Table 1).

Histopathology

This study focused on the examination of FFPE tissue samples from the central nervous system (CNS). Organ samples were collected during necropsy and fixed in 10% neutral buffered formalin (NBF) for at least 24 hours. For histopathological examination, samples were processed routinely and sections were stained with Hematoxylin and eosin (HE).

RNA Extraction and RT-qPCR

Total RNA from FFPE brain sections was extracted using the miRNeasy FFPE kit (Qiagen, Hilden, Germany) following the manufacturer's instructions. During the RNA extraction, the preparations were spiked with a defined copy number of in vitro-transcribed RNA of the eGFP gene to serve as an extraction and amplification control during reverse transcription quantitative PCR (RT-qPCR), as described previously (*2*).

Rustrela virus (RusV) RNA was detected by the specific RT-qPCR assay panRusV-2 targeting the consensus sequence for the detection of 5′ terminus of RusV genomes originating from Germany, Sweden and Austria, as described previously (*3*). Briefly, the panRusV-2 RT-qPCR was performed with AgPath-ID One-Step RT-PCR reagents (Thermo

Fisher Scientific, Waltham, MA, USA), primers RusV_234+ and RusV_323- (final concentration: 0.8 µM each), probe RusV_256_P (0.4 µM), eGFP-specific primers (0.2 µM each) and probe (0.15 µM) (*2*), and 2.5 µL extracted RNA in a total volume of 12.5 µL. All primers and probes are listed in Appendix Table 2. The reaction was performed with the following cycler setup: 45°C for 10 min, 95°C for 10 min, 45 cycles of 95°C for 15 sec, 60°C for 30 sec and 72°C for 30 sec. A standard RNA preparation of a RusV-positive donkey brain (GenBank accession number MN552442.2) (*4*) served as positive control and was used for the calibration of cycle of quantification (Cq) values in each RT-qPCR analysis.

Sequencing and Phylogenetic Analysis

For phylogenetic analysis, partial p150-encoding sequences of 409 nucleotides (nt) length (corresponding to positions 100 to 508 of reference genome MN552442.2) were generated for all three RusV-positive animals by Sanger sequencing of four overlapping RT-PCR amplicons of 142 to 191 base pairs (bp) length. Briefly, 2.5 µl extracted RNA were amplified in a total volume of 25 µl using the SuperScript III One-Step RT-PCR system with Platinum Taq DNA polymerase (Thermo Fisher Scientific, Waltham, MA, USA) and 0.4 µM each of the respective forward and reverse primers (Appendix Table 2). The cycler setup consisted of 50°C for 30 min, 94°C for 2 min, followed by 40 cycles of 94°C for 30 sec, 63°C for 30 sec, and 68°C for 15 sec, and a final elongation step at 68°C for 5 min. Following separation and visualization by gel electrophoresis, amplification products were purified using Zymoclean Gel DNA Recovery Kit (Zymo Research, Freiburg, Germany) and Sanger sequencing service was provided by Eurofins Genomics (Ebersberg, Germany). Overlapping amplicons were sequenced in both directions and consensus sequences were generated after de novo assembly of quality- and primer-trimmed raw sequences in Geneious Prime 2021.0.1 (Biomatters Ltd, Auckland, New Zealand). Sequences are available in GenBank under accession numbers OQ319478 to OQ319480.

Phylogenetic analysis was performed for the sequences generated in this study in combination with all previously published RusV sequences for which the partial p150-encoding sequences of 409 nt length were available in GenBank (n = 49). Following nucleotide sequence alignment using MUSCLE 3.8.425 (available in Geneious Prime 2021.0.1), a Maximum-likelihood (ML) phylogenetic tree was calculated using IQ-TREE version 2.2.0 (TIM2+F+G4 with 1,000 bootstrap replicates) (*5*).

Immunohistochemistry (IHC)

Appendix Table 3 provides an overview of primary antibodies used in this study, their target structure as well as information about their clonality, host species, performed antigen

retrieval and the source. Immunohistochemistry was performed as previously described (*6*). Briefly, deparaffinization and rehydration was followed by inhibition of endogenous peroxidase activity by incubation in 85% ethanol and 0.5% hydrogen peroxidase for 30 min at room temperature. After washing in phosphate-buffered saline (PBS), heat-induced epitope retrieval was performed by using the respective buffer in a microwave at 800 W for 20 min (Appendix Table 3). For labeling with antibody 9D5, sections were incubated with Proteinase K [1000 ml PBS admixed with 3 µl Proteinase K (20 mg/mL, Roche Diagnostics, Mannheim, Germany)] for 7 min at room temperature. Subsequent washing in PBS was followed by reducing unspecific binding reaction by incubation with inactivated normal goat serum (diluted 1:5 in PBS) for 30 min at room temperature. Primary antibodies were diluted in PBS with addition of 1% bovine serum albumin. Afterwards, sections were incubated with primary antibodies in their respective concentration at 4°C overnight (Appendix Table 3). Negative controls were generated by replacement of the primary antibody with serum of Balb/c mice. After washing in PBS, a biotinylated goat-anti mouse antibody (diluted 1:200 in PBS) was applied and incubated for 60 min at room temperature. Afterwards, the avidin-biotin-peroxidase complex (ABC, Vectastain ABC Kit Standard, Vector Laboratories, Burlingame, USA) was added for 30 min at room temperature. For visualization of immunopositive staining, incubation of ABC was followed by the application of 3,3-diaminobenzidine tetrahydrochloride (0.05%, Sigma Aldrich Chemie GmbH, Darmstadt, Germany) with 0.03% hydrogen peroxide for 5 min at room temperature. Finally, sections were dehydrated and subsequently counterstained with Mayer´s hematoxylin (Roth C. GmbH & Co KG, Karlsruhe, Germany).

In Situ Hybridization (ISH)

ISH was performed by using the ViewRNA ISH Tissue Core Kit (Invitrogen by Thermo Fisher Scientific, Vienna, Austria) and a commercially produced probe (ViewRNA Type 1 probe set, Life Technologies GmbH, Darmstadt, Germany). The probe was designed on the partial p150-encoding RusV sequence available from lions 2 and 3 (GenBank accession numbers OQ319479 and OQ319480). Experimental procedure was performed according to the manufacturer´s protocol with minor variations (*7*). The sections were heated in a dry oven at 60°C for one hour the day before ISH was performed. After deparaffinization and rehydration, sections were incubated in Pretreatment Solution at 85–90°C for 10 or 20 min, depending on the type of tissue. After performing several washing steps in autoclaved double-distilled water and PBS, protease digestion and fixation was achieved by incubation of the sections in protease solution (protease diluted 1:100 in PBS) for 10 min at 40°C.

Afterwards, sections were washed twice in PBS and fixed in 10% NBF for 4 min at room temperature. Using the standard protocol, a positive signal could not be obtained in any animal by ISH. By extending the hybridization time from 2 hours to 4 hours and the application of an additional pretreatment with hydrochloric acid (0.2 M) for 10 min at room temperature, positive reactions were observed. Sections were hybridized with the probe diluted 1:25 in Probe Set Diluent at 38°C. For negative controls, only Probe Set Diluent was applied. Signal detection and amplification was achieved by subsequent incubation with Pre-amplifier Mix, Amplifier Mix and Label Probe 1-AP Solution (diluted 1:500) at 40°C and subsequent application of AP Enhancer Solution for 5 min at room temperature. Finally, sections were stained by incubation with Fast Red Staining Solution for 60 min at 40°C. Counterstaining was performed with Mayer´s hematoxylin (Roth C. GmbH & Co KG).

Appendix Table 1. Detection of rustrela virus in tissue from lions with and without nonsuppurative meningoencephalitis*

					Detection of RusV RNA or antigen			IHC for dsRNA		
No.	Internal ID	Sex	Histopathologic lesions in the CNS	Tested tissue	RT-qPCR Cq value	IHC	ISH	K1	J2	9D5
1	S6659/80	F	Mild, multifocal, lymphohistiocytic ME and vasculitis	Cerebrum, cerebellum Liver, spleen	**31, 32** ND	**Pos** ND	Neg Neg	**Pos** ND	**Pos** ND	Neg ND
2	S6076/89	F	Mild, multifocal, lymphohistiocytic ME and vasculitis	Cerebrum, cerebellum Liver, thyroid gland, lung, pancreas, adrenal gland, heart, stomach, urinary bladder	**30, 38** ND	**Pos** ND	**Pos** Neg	**Pos** ND	**Pos** ND	Neg ND
3	S6077/89	M	Mild, multifocal, lymphohistiocytic ME and vasculitis	Cerebrum, cerebellum Kidney, liver, stomach, thymus, urinary bladder, lung, adrenal gland, spleen, heart	**29, 29** ND	**Pos** ND	**Pos** Neg	**Pos** ND	**Pos** ND	Neg ND
4	S96/06	F	No significant lesions	Cerebrum, cerebellum	Neg	Neg	ND	**Pos**	**Pos**	Neg
5	S692/06	F	No significant lesions	Cerebrum, cerebellum	Neg	Neg	ND	**Pos**	**Pos**	Neg
6	S303/14	M	No significant lesions	Cerebrum, cerebellum	Neg	Neg	ND	**Pos**	**Pos**	Neg
7	S1085/16	F	No significant lesions	Cerebrum, cerebellum Spleen, adrenal gland, liver, thyroid gland, pituitary gland, kidney, urinary bladder, diaphragm, tongue, pancreas, lung, stomach, intestine, bone marrow, heart, mesenterial lymph node, lung lymph node	Neg ND	Neg ND	ND Neg	**Pos** ND	**Pos** ND	**Pos** ND
8	S303/19	F	No significant lesions	Cerebrum, cerebellum	Neg	Neg	ND	**Pos**	**Pos**	Neg
9	S885/20	F	No significant lesions	Cerebrum, cerebellum	Neg	Neg	ND	**Pos**	**Pos**	**Pos**
10	S342/21	F	No significant lesions	Cerebrum, cerebellum	Neg	Neg	ND	**Pos**	**Pos**	Neg
11	S32/22	M	No significant lesions	Cerebrum, cerebellum	Neg	Neg	ND	**Pos**	**Pos**	Neg

*Bold text indicates positive result. CNS, central nervous system; Cq, cycle of quantification; dsRNA, double-stranded RNA; F, female; IHC, immunohistochemistry; ISH, in situ hybridization; M, male; ME, meningoencephalitis; ND, not done; Neg, negative; Pos, positive; RT-qPCR, reverse transcription quantitative PCR; RusV, rustrela virus.

Appendix Table 2. Primers and probes used in study of rustrela virus in lions with nonsuppurative meningoencephalitis*

Assay	Primer/probe	Sequence (5′ to 3′)	Reference
panRusV-2	RusV_234+	CCCCGTGTTCCTAGGCAC	Matiasek et al. (*3*)
	RusV_256_P	FAM-GTGAGCGACCACCCAGCACTCCA-BHQ1	Matiasek et al. (*3*)
	RusV_323-	TCGCCCCATTCWACCCAATT	Matiasek et al. (*3*)
eGFP mix 1	EGFP-1-F	GACCACTACCAGCAGAACAC	Hoffmann et al. (*2*)
	EGFP-Probe1_HEX	HEX-AGCACCCAGTCCGCCCTGAGCA-BHQ1	Hoffmann et al. (*2*)
	EGFP-2-R	GAACTCCAGCAGGACCATG	Hoffmann et al. (*2*)
Conventional RT-PCR & Sanger sequencing	RusV_80+	GTCGAGGAGCAGATAAGCCC	Matiasek et al. (*3*)
	RusV_248-	TGCCTARGAACACGGGGCG	This study
	RusV_182+	GARTGCATGAGCGCCGAAGG	This study
	RusV_323-	TCGCCCCATTCWACCCAATT	Matiasek et al. (*3*)
	RusV_227+	CCGCGCCCCGTGTTCYTAGG	This study
	RusV_382-	CCGYTGGGCGAGGCGTADSA	This study
	RusV_338+	TGCCTVGTBAACCCCAGCCC	This study
	RusV_528-	AGCGYCGGGTCYGTVACAAC	This study

*RT-qPCR, reverse transcription quantitative PCR; RusV, rustrela virus.

Appendix Table 3. Overview of primary antibodies used in study of lions with rustrela virus*

Antigen	Target structure	Clonality species	Dilution	Antigen retrieval	Reference
2H11B1	RusV capsid protein	Monoclonal mouse	1:100	Microwave; citrate buffer	Matiasek et al. (*3*)
K1	dsRNA	Monoclonal mouse	1:150	Microwave; citrate buffer	Störk et al. (*6*)
J2	dsRNA	Monoclonal mouse	1:300	Microwave; citrate EDTA buffer	Störk et al. (*6*)
9D5	dsRNA	Monoclonal mouse	1:100	Proteinase K	Störk et al. (*6*)

*dsRNA, double-stranded RNA; EDTA, ethylendiamintetraacetate; RusV, rustrela virus.

References

1. Truyen U, Stockhofe-Zurwieden N, Kaaden OR, Pohlenz J. A case report: encephalitis in lions. Pathological and virological findings. Dtsch Tierarztl Wochenschr. 1990;97:89–91. PubMed

2. Hoffmann B, Depner K, Schirrmeier H, Beer M. A universal heterologous internal control system for duplex real-time RT-PCR assays used in a detection system for pestiviruses. J Virol Methods. 2006;136:200–9. PubMed https://doi.org/10.1016/j.jviromet.2006.05.020

3. Matiasek K, Pfaff F, Weissenböck H, Wylezich C, Kolodziejek J, Tengstrand S, et al. Mystery of fatal “staggering disease” unravelled: novel rustrela virus causes severe meningoencephalomyelitis in domestic cats. Nat Commun. 2023;14:624. PubMed https://doi.org/10.1038/s41467-023-36204-w

4. Bennett AJ, Paskey AC, Ebinger A, Pfaff F, Priemer G, Höper D, et al. Relatives of rubella virus in diverse mammals. Nature. 2020;586:424–8. PubMed https://doi.org/10.1038/s41586-020-2812-9

5. Minh BQ, Schmidt HA, Chernomor O, Schrempf D, Woodhams MD, von Haeseler A, et al. IQ-TREE 2: New Models and Efficient Methods for Phylogenetic Inference in the Genomic Era. Mol Biol Evol. 2020;37:1530–4. PubMed https://doi.org/10.1093/molbev/msaa015

6. Störk T, de le Roi M, Haverkamp AK, Jesse ST, Peters M, Fast C, et al. Analysis of avian Usutu virus infections in Germany from 2011 to 2018 with focus on dsRNA detection to demonstrate viral infections. Sci Rep. 2021;11:24191. PubMed https://doi.org/10.1038/s41598-021-03638-5

7. Postel A, Hansmann F, Baechlein C, Fischer N, Alawi M, Grundhoff A, et al. Presence of atypical porcine pestivirus (APPV) genomes in newborn piglets correlates with congenital tremor. Sci Rep. 2016;6:27735. PubMed https://doi.org/10.1038/srep27735